Matrix Biology Plus 23 (2024) 100159

Contents lists available at ScienceDirect

Matrix Biology Plus

journal homepage: www.sciencedirect.com/journal/matrix-biology-plus

Matrisome proteomics reveals novel mediators of muscle remodeling with aerobic exercise training

Pattarawan Pattamaprapanont [a,b], Eileen M. Cooney [a], Tara L. MacDonald [a,b], Joao A. Paulo [c], Hui Pan [a], Jonathan M. Dreyfuss [a,b], Sarah J. Lessard [a,b,*]

[a] Research Division, Joslin Diabetes Center, Boston, MA, USA
[b] Harvard Medical School, Boston, MA, USA
[c] Department of Cell Biology, Harvard Medical School, Boston, MA 02115, USA

ARTICLE INFO

Keywords:
Exercise
Skeletal muscle
Proteomics
Remodeling
Core matrisome
Matrisome-associated

ABSTRACT

Skeletal muscle has a unique ability to remodel in response to stimuli such as contraction and aerobic exercise training. Phenotypic changes in muscle that occur with training such as a switch to a more oxidative fiber type, and increased capillary density contribute to the well-known health benefits of aerobic exercise. The muscle matrisome likely plays an important role in muscle remodeling with exercise. However, due to technical limitations in studying muscle ECM proteins, which are highly insoluble, little is known about the muscle matrisome and how it contributes to muscle remodeling. Here, we utilized two-fraction methodology to extract muscle proteins, combined with multiplexed tandem mass tag proteomic technology to identify 161 unique ECM proteins in mouse skeletal muscle. In addition, we demonstrate that aerobic exercise training induces remodeling of a significant proportion of the muscle matrisome. We performed follow-up experiments to validate exercise-regulated ECM targets in a separate cohort of mice using Western blotting and immunofluorescence imaging. Our data demonstrate that changes in several key ECM targets are strongly associated with muscle remodeling processes such as increased capillary density in mice. We also identify LOXL1 as a novel muscle ECM target associated with aerobic capacity in humans. In addition, publically available data and databases were used for in silico modeling to determine the likely cellular sources of exercise-induced ECM remodeling targets and identify ECM interaction networks. This work greatly enhances our understanding of ECM content and function in skeletal muscle and demonstrates an important role for ECM remodeling in the adaptive response to exercise. The raw MS data have been deposited to the ProteomeXchange with identifier PXD053003.

Introduction

Skeletal muscle is the largest organ by mass in healthy individuals, and contributes to essential processes including locomotion, whole-body metabolism, and endocrine signaling [1]. Moreover, muscle health and function is tightly associated with overall health, quality of life, and longevity [2]. Muscle also has a unique ability to remodel within a relatively short timeframe (weeks to months) in response to stimuli such as contraction or exercise [3]. Remodeling processes that typically occur in muscle with aerobic exercise training include changes in fiber-type composition [4] and increases in capillary density via exercise-induced angiogenesis [5]. The phenotypic changes that occur in muscle with training contribute significantly to the well-reported health benefits of exercise [6].

The skeletal muscle extracellular matrix (ECM) is essential for many important muscle functions including muscle contraction, cellular signaling, and energy metabolism [7–10]. This complex compartment is host to a variety of cell types (e.g. muscle progenitor cells, endothelial cells, fibroblasts) that are involved in muscle remodeling processes [11,12]. Remodeling of muscle ECM is associated with disease states such as muscular dystrophy and metabolic disease [13,14], as well as positive muscle adaptations that occur with exercise training [15]. As in other tissues, muscle ECM proteins can be categorized into core components (e.g. collagens, proteoglycans, glycoproteins), as well as associated proteins (e.g. ECM regulators) [16].

There is abundant evidence that exercise training regulates

Abbreviations: ECM, extracellular matrix; ET, exercise-trained; CON, control; TTE, time to exhaustion; TMT, tandem mass tags; NGS, normal goat serum.

* Corresponding author at: Joslin Diabetes Center and Harvard Medical School, One Joslin Place, Boston, MA 02215, USA.
E-mail address: sarah.lessard@joslin.harvard.edu (S.J. Lessard).

https://doi.org/10.1016/j.mbplus.2024.100159
Received 25 April 2024; Received in revised form 29 July 2024; Accepted 30 July 2024
Available online 7 August 2024

transcription of skeletal muscle ECM components [17]. However, altered transcript levels may not accurately reflect actual remodeling events of muscle ECM proteins in response to exercise. This is because the content of ECM proteins can also be modulated by protein synthesis rates, post-translational modification, and breakdown by proteolytic enzymes [18–20]. In addition, the physiological environment of the host can alter the rates of these processes, changing the half-life of ECM proteins through processes like cross-linking and glycation [21].

There is also data demonstrating that exercise can alter components of the muscle proteome, including some ECM proteins [22]. However, analysis of the precise protein make-up of ECM components, or "matrisome", of muscle and other tissues has been challenging due to the large size, extensive post-translational modification, and insoluble nature of the proteins [23]. Consequently, traditional methodologies to extract and quantify muscle proteins may not provide comprehensive coverage of the muscle proteome. Fortunately, recent advances in proteomic methodology have led to an enhanced understanding of ECM composition of skeletal muscle and other tissues [24,25]. To date, much of the work done to examine the muscle matrisome using ECM-specific extraction techniques has been performed in sedentary rodents. Determining how exercise, which is a critical regulator of muscle health and function, can regulate the muscle matrisome, is a key unanswered question.

The aim of our investigation was to utilize ECM-specific proteomic techniques to determine how aerobic exercise training regulates remodeling of the skeletal muscle matrisome. In addition, we aimed to determine how ECM remodeling with exercise relates to functional changes in muscle phenotype that impact health, such as exercise-induced increases in muscle capillary density. Our results demonstrate that a substantial proportion of the muscle matrisome is altered by exercise training. We demonstrate that matrisome remodeling is tightly associated with exercise-induced changes in muscle phenotype- identifying potentially novel regulators of the adaptive response to exercise. In addition, we identify muscle ECM proteins in mouse and human skeletal muscle that have not previously been investigated.

Results

Utilizing an ECM enrichment method developed for ovarian tissue and optimized for skeletal muscle, we identified 225 ECM proteins from mouse gastrocnemius muscle which represent 4% and 7% of all proteins quantified from the soluble and insoluble fractions of our skeletal muscle samples (Fig. 2A). After combining proteins that were found in both fractions or had duplicate Uniprot protein IDs, a total of 161 ECM proteins were identified in muscle (Fig. 2B). Of these, 76 proteins were core-matrisome and 85 proteins were ECM-associated proteins (Table 1). A greater extent of ECM-associated proteins were found in the soluble fraction (80 soluble vs 29 insoluble), whereas a similar proportion of core matrisome proteins were found in both fractions (52 soluble vs 64 insoluble). The most abundant core matrisome component quantified were glycoproteins (64%), followed by collagens (20%) and proteoglycans (16%). In the matrisome-associated category, more than 50% were categorized as ECM regulators and others were identified as ECM–affiliated (28%) and secreted factors (18%). Some of our identified ECM proteins have been previously recognized as major muscle ECM components (COL1A1, FBN1, FN1) or muscle ECM regulators (MMP2, GPC1, MSTN). However, some of our identified ECM proteins have not been previously reported in muscle (e.g. COL9A3, GPC4, S100A16).

To determine how exercise training impacts muscle ECM remodeling, a cohort of mice underwent 6-weeks of voluntary wheel running, while controls remained sedentary. Exercise-trained mice ran 552±33 km over the training period, and had lower body weight compared to sedentary controls (Supplementary Fig. 1A–B). Exercise-trained mice significantly improved their aerobic exercise capacity, expressed as time to exhaustion, compared to controls, indicating that training produced the anticipated physiological adaptations (Supplementary Fig. 1C).

Table 1
Annotated matrisome proteins identified in mice gastrocnemius muscle using two-fraction MS-compatible methodology. Identified proteins were found in all samples (N=11), regardless of experimental group. Annotations are taken from the Naba matrisome database.

Categories	Divisions	Matrisome protein name
Core Matrisome Proteins	Collagens	COL15A1, COL5A3, COL18A1, COL14A1, COL3A1, COL6A2, COL4A1, COL6A1, COL6A6,COL4A2, COL12A1, COL9A3, COL1A1, COL6A3, COL6A5
	ECM Glycoproteins	VWF, MFAP5, FBN1, LAMA4, FBLN5, DPT, MFAP1A, FN1, TNXB, POSTN, NID1, TINAGL1, LAMB2, MFAP2, LAMC1, TGFBI, MFAP4, LAMB1, LAMA2, FBLN1, LAMA5, VTN, FGG, PXDN, CILP2, CILP, THBS4, FGB, ADIPOQ, LAMA1, PCOLCE, NID2, FGA, MFGE8, TNC, THBS1, AEBP1, EFEMP1, SMOC2, CRELD2, CRELD1, COMP, VIT, ECM1, ABI3BP, LRG1, VWA5A, FNDC1, THBS3
	Proteoglycans	HSPG2, DCN, LUM, PRELP, ASPN, PRG4, OGN, BGN, FMOD, CHAD, KERA, VCAN
ECM-Associated Proteins	ECM regulators	PLG, SERPINA3K, LOXL1, TRY4, SERPINA1A, SERPINH1, CTSD, AMBP, PZP, TGM2, ITIH3, MMP2, AGT, SERPING1, ITIH1, CTSB, SERPINB1A, SERPINE2, CTSA, TRY10, SERPIND1, CTSL, F13A1, SERPINA1C, SERPINC1, FAM20B, SERPINA6, CTSC, ITIH2, SERPINF1, MUG2, HRG, ITIH4, CTSZ, SERPINB9, OGFOD1, P4HA1, PLOD1, F2, SERPINA1D, SERPINA1B, SERPINF2, CST3, SERPINA3N, CPN2, KNG1
	ECM-affiliated Proteins	ANXA4, ANXA11, CSPG4, ANXA5, ANXA2, MBL2, ANXA1, LGALS1, HPX, ANXA3, ANXA7, ANXA6, GPC4, SEMA3C, GPC6, GPC1, LGALSL, CLEC2D, CLEC10A, CLEC3B, EMCN, LMAN1, C1QA, SEMA7A
	Secreted factors	HBEGF, ANGPTL7, S100A6, S100A10, S100A4, CCBE1, S100A13, CTF1, S100A9, FGF1, MSTN, HCFC1, S100A11, FGF13, S100A16

Using our newly optimized ECM enrichment and quantification methods, we found that exercise altered more than 34% of identified core matrisome proteins, with the majority being increased by training (Fig. 3A–B). A complete list of quantified ECM proteins from the soluble and insoluble fractions, and how they were altered by exercise training appears in Supplementary File 1. For example, MFAP5 and FBN1 were increased by 2.0- and 1.9-fold, respectively, in response to exercise training. On the other hand, matrisome-associated proteins were more likely to decrease with exercise training (Fig. 3A–B). Overall, our findings demonstrate a profound remodeling of core and matrisome-associated proteins in muscle induced by aerobic exercise training.

Spearman correlation analysis identified 34 muscle ECM proteins that are associated (rho$\geq$ 0.5, P$\leq$0.1) with improvements in exercise capacity (ΔTTE) with exercise training (Table 2). Some targets were negatively correlated (e.g. HSPG2, COL9A1) and others were positively correlated (e.g. FBLN5, FN1) with ΔTTE. These data suggest that muscle ECM composition may play an important role in the physiological adaptations to exercise. This is likely because changes in muscle phenotype make important contributions to the overall health benefits of exercise, including improved exercise capacity [26,27].

To determine whether ECM targets we identified to be exercise-regulated via proteomics are associated with key changes in muscle phenotype, we performed a second exercise-training study in a larger (N=12 sedentary and N=12 exercise-trained) cohort of mice. Exercise-trained mice were housed in voluntary wheel-running cages and ran ~429±41 km over the course of 6-weeks (Supplementary Fig. 2A). Exercise produced expected physiological adaptations such as reduction in body weight (Supplementary Fig. 2B) and improved aerobic exercise

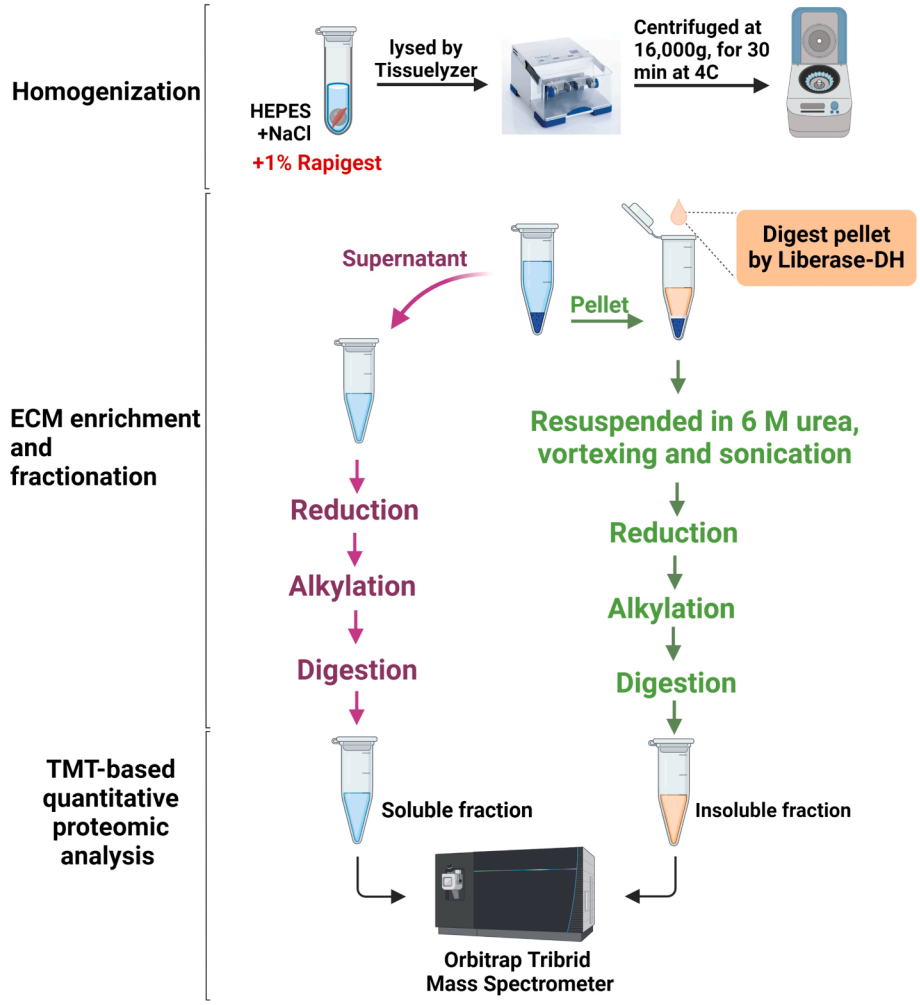

Fig. 1. Experimental workflow for the quantification of the skeletal muscle matrisome. 10 mg of pulverized gastrocnemius muscle was lysed with NaCl and Rapigest with mechanical disruption. The lysate was centrifuged to separate the supernatant (soluble fraction) from the pellet (insoluble fraction). The insoluble fraction was further digested and solubilized, and both fractions underwent reduction, alkylation and digestion for mass spectrometry. Peptides were labeled by tandem mass tags (TMT), fractionated, and analyzed by LC-MS3. Figure created with Biorender.com.

capacity (Supplementary Fig. 2C), demonstrating a robust exercise training stimulus. Improved aerobic capacity with training is frequently associated with increases in skeletal muscle capillary density and a shift toward a more oxidative (type 2A) fiber-type [4,5]. These adaptations can contribute to improved aerobic capacity by enhancing oxygen delivery and utilization by working muscles [26]. Accordingly, we also found that skeletal muscle phenotype was altered by exercise, with trained mice displaying a more oxidative fiber type (Supplementary Fig. 2D) and increased capillary density (Supplementary Fig. 2E) in gastrocnemius muscle compared to sedentary controls.

Next, we validated a subset of core matrisome and matrisome-associated proteins identified to be exercise-regulated by MS analysis in this independent cohort of mice. We selected ECM proteins from both core-matrisome and matrisome-associated divisions. Availability of a validated antibody against mouse proteins was also a criterion for selection. Some selected proteins have been shown to be key ECM remodeling regulators [e.g. Lysyl oxidase like1 (LOXL1) and Plasminogen (PLG)], or main ECM structural components [e.g. Fibronectin1 (FN1, muscle ECM) and Fibrillin1 (FBN1, Elastin)]. Other selected proteins have a currently unknown role in muscle [e.g. Laminin subunit alpha4 (LAMA4), Semaphorin 3C (SEMA3C) and Tubulointerstitial nephritis antigen-like 1 (TINAGL1)]. Consistent with MS analysis, immunoblot analysis revealed that exercise training regulates the muscle levels of several core matrisome proteins (e.g. FBN1, TINAGL1, LAMA4; Fig. 4A and C) and matrisome-associated proteins (e.g. PLG, SEMA3C, LOXL1; Fig. 4B and D). Western blotting of muscle LOXL1 demonstrated several bands upregulated by exercise. LOXL1 is produced as a pre-proenzyme and undergoes post-translational modification and cleavage to produce a 32 kDa active enzyme [28], which is the band that we quantified for our analysis. These data demonstrate that a subset of ECM targets we discovered to be regulated by exercise in muscle may be detected by MS-based or blot-based methodologies, and that our results are reproducible in independent cohorts of mice.

For two additional targets, we performed immunofluorescence staining to verify their altered expression with exercise and tissue localization. FN1 is a major component of skeletal muscle ECM. It plays an important role in cell communication by binding with cell surface ligands [29]. Consistent with our MS analysis, immunofluorescence staining demonstrated increased FN1 content in trained-mice muscle in the extracellular space surrounding muscle fibers (Fig. 5A). We next analyzed LAMA4 content and localization. MS and immunoblot analysis showed that LAMA4 was increased by exercise training. However, the major laminin isoform in muscle cell basement membrane is LAMA211 [30], which does not include LAMA4. As LAMA4 is a major basement membrane component of endothelial cells [31], we hypothesized that higher LAMA4 expression in trained-mice would be associated with increased muscle capillary density. In support of this, exercise training increased ECM LAMA4 staining, and LAMA4 was co-localized with

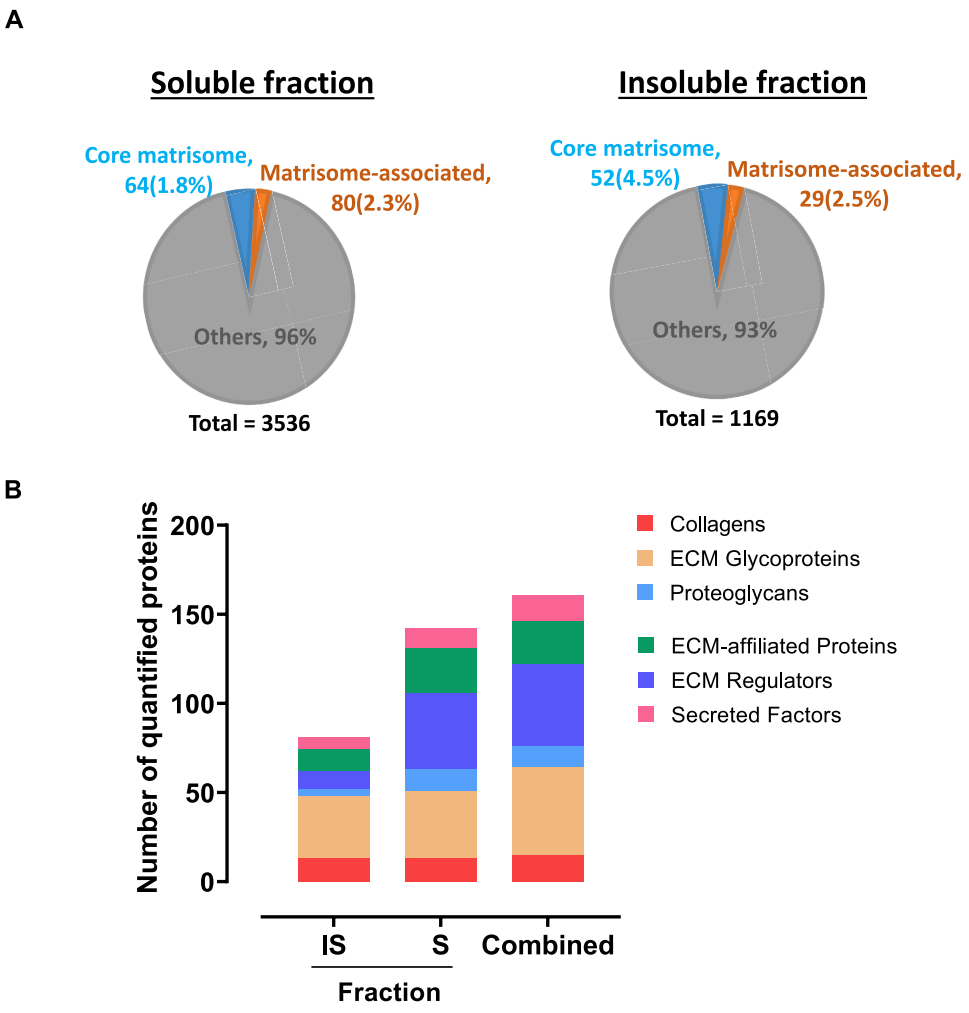

Fig. 2. Skeletal muscle matrisome quantification. (A) Matrisome proteins were annotated from the soluble (left) and insoluble (right) fractions of N=11 mouse gastrocnemius muscles. (B) ECM proteins from the core matrisome (collagens, glycoproteins, proteoglycans) and ECM associated (ECM regulators, ECM-affiliated, secreted factors) categories were identified in muscle by our ECM fractionation protocol.

endothelial cells stained by griffonia lectin (Fig. 5B). Indeed, the number of endothelial cells in each section was significantly correlated with the number of LAMA4 positive cells (Fig. 5C). Interestingly, muscle capillary density and LAMA4 staining were also significantly correlated to the proportion of oxidative muscle fibers, indicating that increases in capillary density and other aspects of muscle remodeling are co-regulated with ECM alterations (Fig. 5D).

To determine whether other ECM components regulated by exercise may be involved in exercise-induced angiogenesis, we performed additional correlation analysis. FBN1, PLG, TINAGL1, LOXL1, SEMA3C and FN1 levels were all significantly and positively correlated with muscle capillary density (Fig. 6A–G). In contrast, none of these targets (aside from LAMA4; Fig. 5) were associated with muscle oxidative fiber composition. Overall, these data identify several specific targets of exercise-induced muscle remodeling that may regulate the critical process of exercise-induced increases in capillary density. We selected a smaller subset of MS-identified exercise-regulated ECM proteins for follow-up analysis. Therefore, it is possible that other, unselected proteins are involved in muscle fiber-type remodeling, as well as other muscle remodeling events, in response to exercise training.

In addition to mature muscle fibers, other cell populations may contribute to skeletal muscle ECM composition. To determine which cell types may be responsible for exercise-induced muscle ECM remodeling, we analyzed the expression of exercise-regulated ECM target genes from three published single-nuclei RNA sequencing datasets [32–34]. The expression pattern of ECM genes in skeletal muscle among various cell types was similar in all three datasets (Fig. 7). Surprisingly, muscle myonuclei were not found to be the primary source of any exercise-regulated ECM targets. Two of the seven genes analyzed, Sema3c and Plg, were expressed in myonuclei, albeit to a lower extent than other, non-muscle nuclei. Among non-muscle nuclei, our subset of exercise-regulated ECM genes are predominantly expressed in fibro-adipogenic progenitor cells (FAPS; Fig. 7).

Consistent with our immunofluorescence analysis demonstrating co-localization of LAMA4 protein and capillaries, endothelial cells were found to be a source of Lama4 gene expression. However, single nucleus RNA-sequencing analysis demonstrated that adipocytes and FAPS may also be significant sources of LAMA4. Whether these cell types, like endothelial cells, are a significant source of LAMA4 protein is unknown, as RNA levels do not always accurately reflect protein content of a tissue. Our data suggest endothelial cells are the primary source of LAMA4 protein in muscle, which is in line with observations in tumors [35]. Another protein target we found to be tightly associated with muscle capillary density, TINAGL1, was expressed at the RNA level primarily in endothelial cells and pericytes, which are both known regulators of vascular remodeling. Taken together, these data demonstrate the critical role of non-muscle cells in exercise-regulated ECM remodeling and changes in muscle phenotype.

Our results demonstrate that several of our exercise-regulated ECM target proteins are associated with muscle capillary density. To

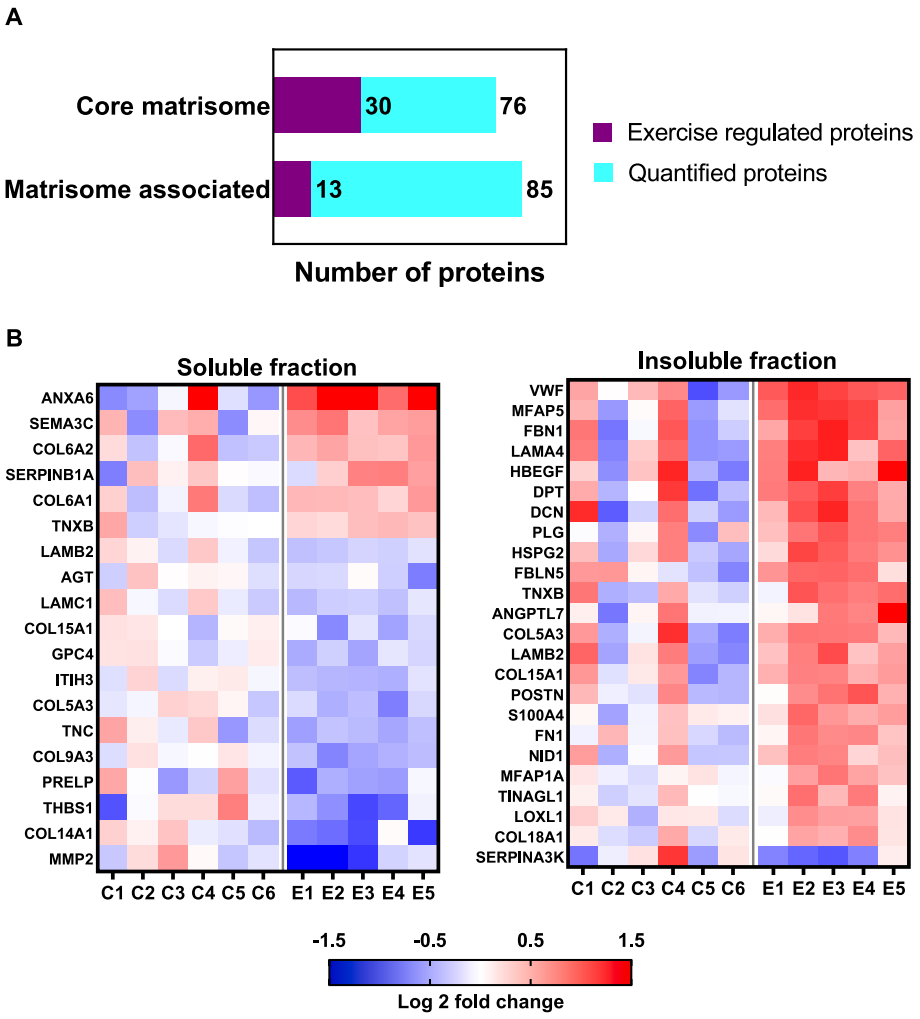

Fig. 3. Regulation of the muscle matrisome by exercise training. (A) Exercise training induced significant remodeling of mouse gastrocnemius ECM in both the core matrisome (30/76; 40%) and ECM-associated proteins (13/85; 15%). (B) Heat map demonstrates log2 fold change of ECM proteins that are altered by exercise from soluble (left) and insoluble (right) fractions in Control (C1-C6) and Exercise-trained (E1-E5) mice. Only proteins with >1.2 fold-change and P-value <0.1 by moderated t-tests (sedentary vs. exercise-trained) are shown in the heat map.

determine whether these targets may interact to mediate exercise-associated muscle remodeling, we utilized the Extracellular Matrix Interaction Database, MatrixDB, to analyze interactions between our exercise-regulated ECM targets. Networks involving 72 ECM proteins were found to have at least one member regulated by exercise in skeletal muscle (Fig. 8). Notably, LOXL1, FBN and FN1, three exercise-induced ECM target proteins that we found to be associated with muscle capillary density, are in the same network (Fig. 8; Top left). LAMA4, which was also found to be linked to muscle capillary density, was part of a larger, independent network along with 7 other MS-identified exercise-regulated targets (NID1, THBS1, COL15A1, COL6A1, COL6A2, LAMC1). Notably, the two largest exercise-regulated networks contain both up- and down-regulated proteins, indicating a coordinated and complex response to training. These results identify key ECM-ECM interactions involved in muscle remodeling with exercise training.

We next analyzed human skeletal muscle lysates to determine if ECM targets identified in mice may also be associated with functional phenotypes in humans. We used Western blotting to measure the levels of two proteins, Plasminogen (PLG) and LOXL1, which were shown to be regulated by exercise in mice. These targets were chosen because they were demonstrated in mice to be associated with muscle remodeling with exercise (Fig. 6), and because the antibodies were targeted against a common peptide sequence between mice and humans. PLG and LOXL1 were both detected in muscle lysates from human participants (Fig. 9A). To determine whether PLG and LOXL1 are associated with functional phenotypes in humans, their muscle protein levels were correlated with several metabolic health markers: BMI, glucose tolerance, insulin sensitivity; VO_2peak. Muscle PLG was not significantly associated with any of the analyzed health markers in human participants. In contrast, the mature (32 kDa) form of LOXL1 demonstrated significant positive associations with VO_2peak (mL/kg/ min; Fig. 9B) and siOGTT (Fig. 9C), which is a measure of insulin sensitivity derived from an oral glucose tolerance test [36]. Active LOXL1 was negatively associated with BMI (Fig. 9D), and the area under the glucose curve assessed during a glucose tolerance test (Fig. 9E). To our knowledge, LOXL1 protein has not previously been quantified in human skeletal muscle. Our data identify LOXL1 as a component of the human muscle matrisome that is associated with several key health and exercise markers.

Discussion

We utilized a recently-developed methodology for ECM protein extraction [37], combined with multiplexed proteomics technology to identify 161 ECM proteins in mouse skeletal muscle. Moreover, we demonstrate that a significant proportion (~27%) of these ECM proteins are regulated by exercise training. From a functional perspective, exercise-regulated ECM proteins were significantly associated with critical adaptations to exercise including enhanced aerobic capacity,

Table 2
Spearman correlation between ΔTTE and exercise-regulated ECM proteins identified by MS. Proteins with the strongest relationship (Rho>0.5) and highest significance (P≤0.1) are shown. These results indicate that muscle ECM remodeling with exercise can predict a key physiological adaptation to exercise training. N=11 pairs analyzed.

Gene symbol	ρ	P-value
Vwf	0.855	0.00165
Fbln5	0.855	0.00165
Hspg2	−0.809	0.00443
Fn1	0.718	0.0168
Col9a3	−0.709	0.0187
Mfap5	0.682	0.0255
Gpc4	−0.673	0.0281
Itih3	−0.664	0.0309
Ctsa	−0.664	0.0309
Plg	0.655	0.0338
Ctf1	−0.655	0.0338
Lama4	0.627	0.044
Prelp	−0.627	0.044
S100a4	0.609	0.0519
Hbegf	0.609	0.0519
Anxa6	0.609	0.0519
Postn	0.6	0.0562
Sema3c	0.591	0.0607
Dpt	0.591	0.0607
Fbln5	0.582	0.0655
Hspg2	0.582	0.0655
Fbn1	0.573	0.0706
Col15a1	0.573	0.0706
Anxa6	0.573	0.0706
Col6a2	0.564	0.0759
Col18a1	−0.564	0.0759
Ctsb	−0.564	0.0759
Lgalsl	−0.564	0.0759
Gpc6	−0.555	0.0816
Cspg4	0.555	0.0816
Col14a1	−0.545	0.0875
Col15a1	−0.545	0.0875
Thbs1	−0.536	0.0936
Nid1	0.527	0.1

increased muscle capillary density, and a more oxidative muscle fiber type.

Other investigations of the skeletal muscle proteome have detected ECM proteins in mice [38] and humans [22]. However, exploration of the skeletal muscle ECM proteome has been restricted by technical limitations in isolating insoluble and heavily cross-linked ECM proteins, which are not readily extracted and quantified by standard proteomic techniques. As an alternative, some of the literature investigating ECM remodeling in muscle has used RNA expression data [15,17]. However, RNA levels do not always reflect protein content and function, especially for proteins with long half-lives and significant post-translational modification, such as ECM proteins. Methodology to better extract, quantify and categorize the ECM proteome of various tissues was developed by Naba and colleagues [16,25,39]. Since then, other investigators have made progress in developing these methods to specifically quantify the matrisomes of skeletal muscle and other tissues [24,30,37,40].

To our knowledge, our identification of 161 unique ECM proteins in skeletal muscle represents a significant increase in proteome coverage compared to other recent investigations [24,40]. Jacobson et al (2020) quantified 75 and 69 proteins using guanidine hydrochloride or sequential fractionation [24], respectively. Using three sequential extractions, Lofaro et al. (2021) identified 124 ECM proteins in mouse muscle. Deep proteomics of mouse skeletal muscle tissue by Deshmukh et al. (2015) also identified 124 ECM proteins- although this methodology was not specifically designed to isolate the ECM. Thus, the two-fraction methodology has expanded muscle matrisome coverage by ~30% compared to existing methods. Our methodology for skeletal muscle ECM proteomics was adapted from that of Ouni et al., (2020) who developed a two-fraction technique using MS-compatible reagents to analyze the ECM proteome of ovarian tissue [37]. To optimize this protocol for skeletal muscle, we used trial-and-error to determine the tissue processing and reagent conditions that would allow us to gain the largest coverage of the muscle matrisome.

The quantification of two fractions (soluble/insoluble) allowed us to keep many of the soluble ECM-associated proteins that may be lost with traditional ECM enrichment techniques, while also gaining access to highly insoluble core ECM components. Jacobson et al. [24] quantified some collagen isoforms that did not appear in our analysis (e.g. COL2A1, COL5A1, COL22A1), suggesting better coverage of this ECM category using sequential fractionation. However, our analysis had greater coverage of ECM regulators (46 vs. 9), glycoproteins (49 vs. 27), ECM-affiliated proteins (24 vs. 8), and secreted factors (15 vs. 2). Thus, selection of the best methodology for matrisome analysis may depend on the specific ECM category of interest. In addition to analyzing two fractions based on solubility, we employed reversed-phase offline fractionation combined with cutting-edge mass spectrometry equipment to increase our depth of coverage. Thus, it is possible a combination of these factors led to enhanced matrisome coverage in the present study.

In addition to expanding overall matrisome coverage, another benefit of the 2-fraction methodology used in our investigation is that it allows for insight into potential changes in solubility of ECM components. A recent investigation of the muscle ECM proteome utilized a sequential enrichment process (1. NaCl, 2. SDS, and 3. urea/thiourea) to examine changes in the ECM-enriched urea/thiourea fraction with age and exercise [41]. The authors found an enrichment of 25 muscle ECM proteins older (~2 year old) male mice, compared to middle-aged (~1 year-old) mice [41]. However, they noted that overall extraction of proteins in the urea/thiourea fraction was lower in older mice, making interpretation of the results difficult. It was suggested that a change in ECM protein solubility due to glycation or cross-linking may have influenced the extraction of ECM protein from aged mice. In addition, the paper demonstrated no influence of unweighted or weighted wheel running on ECM composition [41], although low training volume in older mice may explain the absence of exercise effects. Using two-fraction methodology, whereby soluble and insoluble components are kept and analyzed separately, we demonstrated that exercise training led to an overall decrease in soluble ECM components, and an increase in the insoluble compartment. Thus, in the context of previous studies, studying both soluble and insoluble fractions, rather than discarding fractions that are less enriched in ECM components may provide valuable information on ECM regulation with age and exercise.

Our investigation demonstrates that significant regulation of the muscle ECM proteome occurs with aerobic exercise training. Follow-up analysis in a separate cohort of sedentary and exercise-trained mice confirmed MS findings, and demonstrated that alternative methodologies such as Western blotting and immunostaining can be used to detect exercise-mediated ECM remodeling. Moreover, our results demonstrate significant associations between muscle ECM remodeling and critical exercise-regulated remodeling events such as increased muscle capillary density. Importantly, using publically available single-nucleus RNA sequencing data, we demonstrate that non-muscle cell types such as endothelial cells and FAPS likely make important contributions to muscle ECM remodeling with exercise. Using in silico data, we also identify ECM-ECM interaction networks that are regulated by exercise training. This work contributes significantly to our understanding of how the matrisome contributes to key remodeling events in skeletal muscle.

Exercise training, and the muscle adaptations that occur with training, are key to maintaining good metabolic health and longevity. In contrast, poor adaptive response to exercise training is associated with increased morbidity and mortality [42–46], and occurs more often in those with metabolic disease [36,47–49]. We and others have discovered links between poor exercise response and ECM remodeling in muscle [15,50,51]. Circulating ECM proteins can also predict adaptive

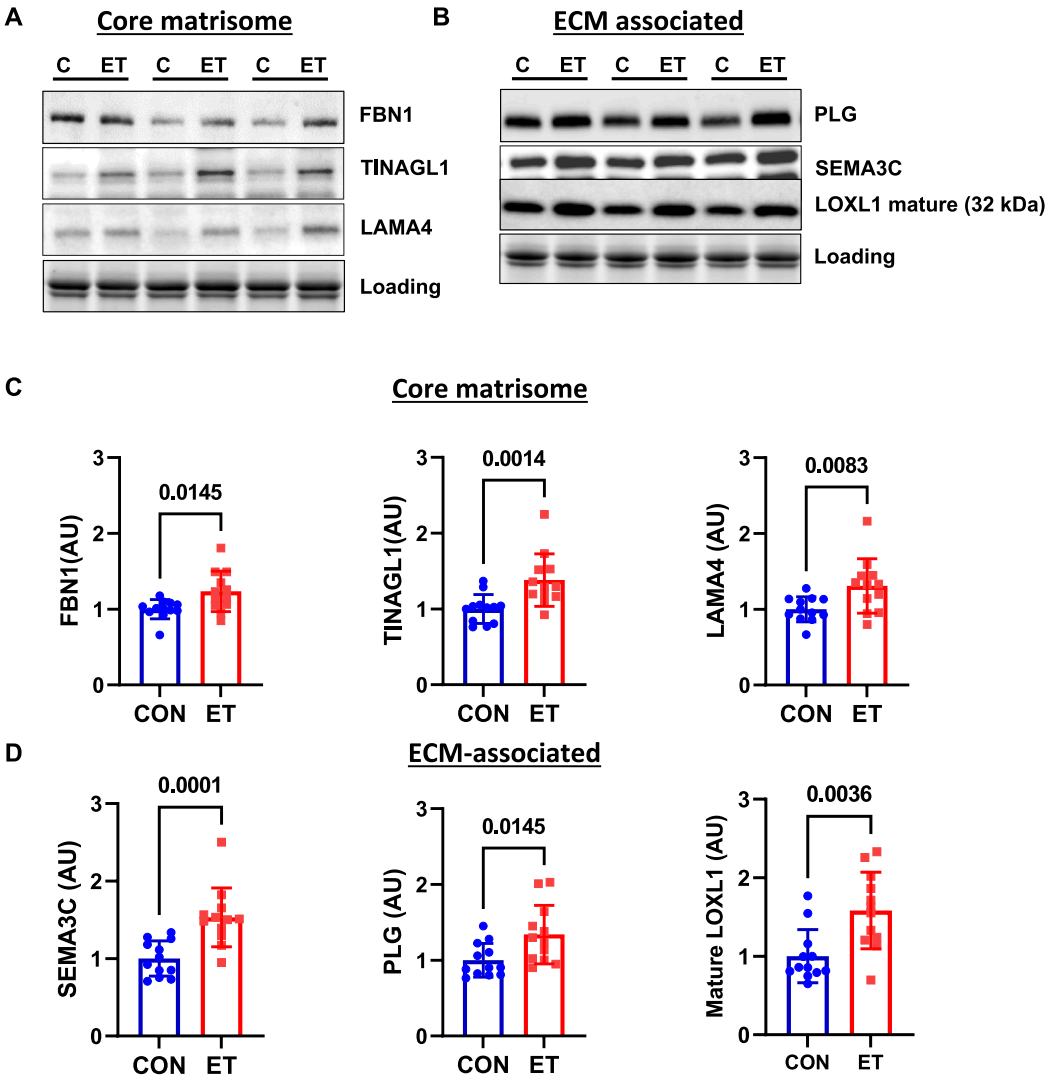

Fig. 4. Western blot analysis of exercise-regulated ECM protein targets identified by MS. (A) A subset of core matrisome, and (B) matrisome-associated proteins were analyzed by Western blotting in the gastrocnemius muscle from sedentary (CON; N=12) and exercise-trained (ET; N=12) mice. These results validated exercise training-induced ECM remodeling of (C) FBN1, TINAGL1, LAMA4, and (D) SEMA3C, PLG, LOXL1. Mean, SD and individuals values are shown. P-value <0.05 by Mann-Whitney U Test was considered statistically significant.

response to aerobic training [52]. Our previous data indicate that aberrant ECM remodeling in low responders to exercise may contribute to blunted exercise-induced angiogenesis [50,51]. However, work to date has used mRNA content or non-specific ECM staining techniques (e.g. wheat germ agglutinin) to quantify ECM changes in muscle associated with low training response. Thus, our data, which identify specific ECM proteins that are regulated by exercise and associated with exercise adaptive responses may have important clinical significance. We anticipate these data will open several new lines of investigation into the mechanisms underlying heterogeneity in the health benefits of exercise.

Many of our validated exercise-regulated proteins were significantly correlated with muscle capillary density (Fig. 6). Some of these targets have been previously associated with angiogenesis in other contexts, including tumor angiogenesis (LOXL1 [53], PLG [54], FN1 [55]), retinal endothelial sprouting (FBN1 [56]), and in vitro tube formation in HUVECs (TINAGL1 [57]). Whole body deletion of TINAGL1 in mice reduced hindlimb muscle size and tended (P=0.07) to decrease soleus muscle capillary to fiber ratio [57]. SEMA3C is a secreted class 3 semaphorin- a class of proteins with known roles in promoting the formation of normal vs. pathological vasculature in disease states such as cancer and retinopathy [58]. We now identify SEMA3C, TINAGL1, and several other angiogenic regulators as being upregulated by aerobic training in mouse skeletal muscle. Some known regulators of exercise-induced angiogenesis such as VEGF have been identified [59]. However, angiogenesis in muscle, as in other tissues, is a complex, multifactorial process regulated by a balance of pro- and anti-angiogenic factors [60]. Our results identify several targets which can be tested as regulators of exercise-induced angiogenesis and muscle remodeling in future studies.

In human skeletal muscle, Hostrup et al. (2022) identified 15 ECM proteins (P<0.1; Baseline vs. Post-Training) regulated by exercise in response to 5 weeks (3 sessions/week) of high-intensity interval training [22]. That study was aimed at investigating changes in the whole proteome and acetylome of skeletal muscle with exercise, and did not utilize methodology to facilitate enrichment or isolation of ECM proteins. The use of ECM-specific methodology may account for identification of a larger number (N=43; P<0.1, fold-change ≥ 1.2; Sedentary vs. Exercise-Trained) of exercise-regulated and total (161 vs. 78) ECM proteins in the present study. Of note, some proteins identified to be regulated in human skeletal muscle by exercise by Hostrup et al. (LAMA4, NID1, TINAGL1, LAMC1) were also found to be regulated by endurance

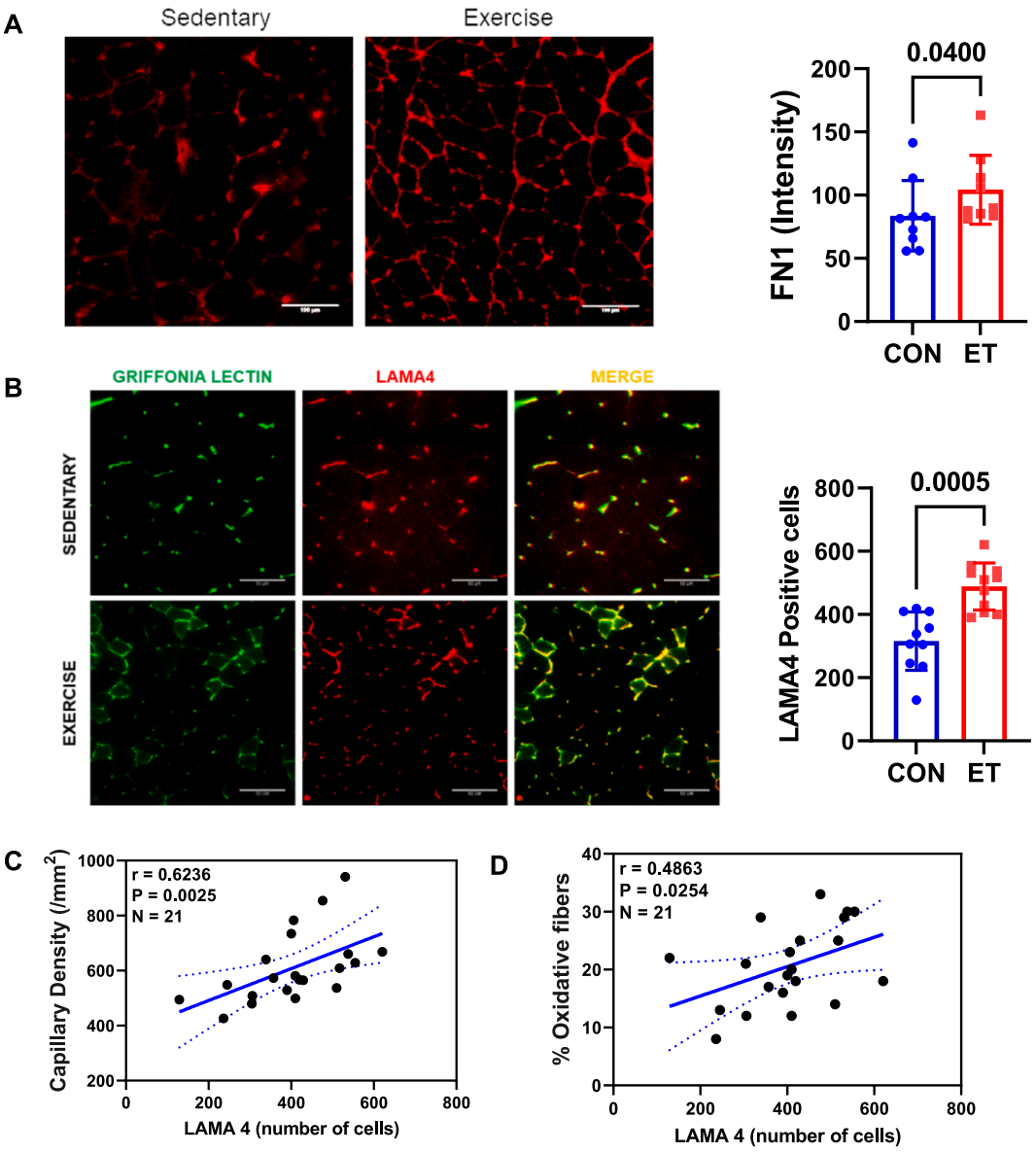

Fig. 5. Validation and localization of exercise-regulated ECM proteins identified by MS. (A) Immunostaining for FN1 confirmed increased protein in the extracellular space of skeletal muscle with exercise training. (B) Training also increased LAMA4 staining in skeletal muscle, and co-localized with endothelial cells stained using griffonia lectin. (C) LAMA4 staining was significantly correlated with muscle capillary density and (D) oxidative fiber-type, suggesting a role in exercise-induced changes in muscle phenotype. Scale bar = 100μm for panel A, 50μm for panel B. P-value < 0.05 by Mann-Whitney U Test was considered statistically significant. Bar graphs demonstrate mean, SD, and individual values. Panels C and D show Spearman correlations and dotted lines represent 95% confidence intervals.

training in our analysis of mouse muscle. Thus, there appears to be good agreement between species for exercise-regulation of muscle ECM proteins. In addition, our follow-up analysis of human skeletal muscle identified LOXL1, which to our knowledge, is a novel target that has not been reported in previous proteomic screens of human or mouse skeletal muscle. We demonstrate significant correlations between higher muscle levels of mature LOXL1 and positive metabolic markers in humans, including VO_2peak, glucose tolerance, and insulin sensitivity.

In summary, our data demonstrate that expanded coverage of the skeletal muscle matrisome can be achieved with a two-fraction MS-compatible multiplexed proteomic approach. Our results establish significant regulation of core matrisome and matrisome-associated ECM components by exercise training. Our data also indicate that these ECM remodeling events with exercise are linked to positive muscle and physiological adaptations resulting from exercise training. Moreover, we identify LOXL1 as an ECM component in human skeletal muscle that is associated with key metabolic health markers and aerobic exercise capacity (VO_2peak). This work represents a significant advance in our knowledge of skeletal muscle matrisome composition and demonstrates an important role for ECM remodeling in the adaptive response to exercise.

Experimental procecures

Animal experiments

All mouse experiments were approved by the Institutional Animal Care and Use Committee of the Joslin Diabetes Center. Male, 8-week-old, CD-1 mice were purchased from Charles River Laboratories (IGS; #022). Mice were group-housed in a pathogen-free facility and maintained on a 12 h normal light/dark cycle with water and food ad libitum. All mice consumed a standard diet (Research Diets, D14020502) consisting of 17% kcal from protein, 73% carbohydrate, and 10% fat. Body weight was measured weekly. Outbred CD-1 mice were used rather than

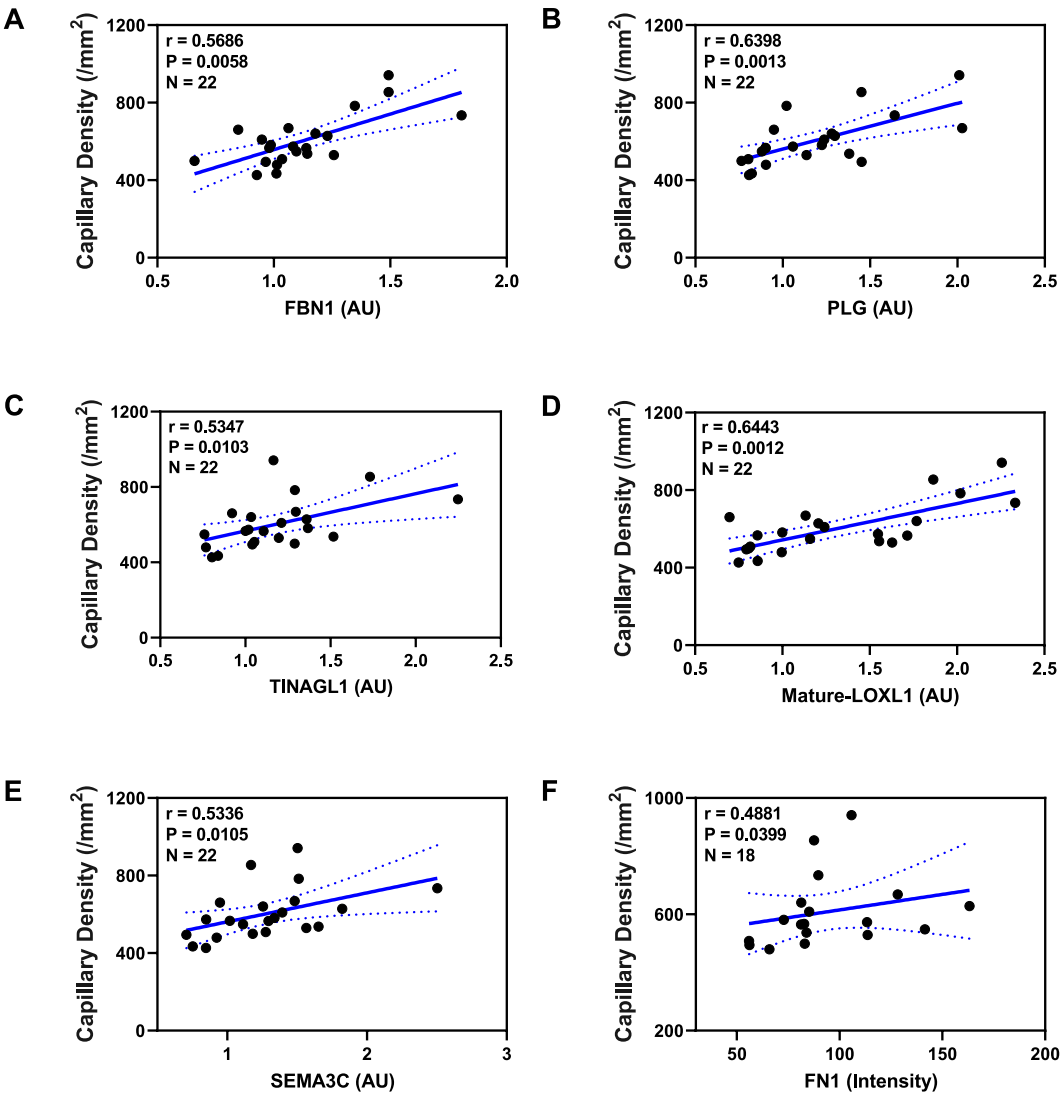

Fig. 6. Correlation between exercise-regulated ECM proteins and capillary density. Expression of (A) FBN1, (B) PLG, (C) TINAGL1, (D) LOXL1 (Mature; 32 kDa), (E) SEMA3C, and (F) FN1 are positively correlated with capillary density- a hallmark of exercise training-induced muscle remodeling. P-value < 0.05 for Spearman correlation was considered statistically significant. 95 % confidence intervals are shown with dotted lines.

inbred strains (e.g. C57BL/6) to increase genetic variance and the likelihood that our results may be translated to humans.

Wheel running

At 16-wks of age, mice were randomly assigned into sedentary and exercise-trained groups. Sedentary mice were group housed in a standard cage with environmental enrichment and were allowed to maintain normal daily activities. Exercise-trained mice were single-housed in a cage with a 4-inch voluntary running wheel for 6 weeks. Voluntary running behavior was recorded in 10 min intervals using a Hall Effect Sensor (0297–0501), Wheel Counter 8 Channel Interface (0297–0050) and a Quad CI-Bus to interface with CI Multi Device Software (v.1.5.5) from Columbus Instruments.

Exercise capacity test

Exercise capacity was measured before and after 6 weeks of voluntary wheel running in exercise-trained mice. Age-matched sedentary control mice were tested alongside exercise-trained mice to control for the effects of age, repeated testing, and experimental conditions on exercise capacity. Before testing, mice were acclimated to a modular treadmill for 2 consecutive days before undergoing aerobic exercise capacity testing to exhaustion using the graded mouse maximal exercise test (GXTm) protocol [61]. Mice were motivated to run with an electrical grid operating at 0.1 mA. Exhaustion was defined as failure to return to the treadmill from the rest platform after three consecutive attempts within the last minute of running. Exercise capacity was expressed as time to exhaustion (TTE). In exercise-trained mice, access to running wheels was restricted for ~24 h before testing.

Identification of exercise-induced muscle ECM remodeling proteins

Sample ECM enrichment and fractionation

To quantify ECM proteins in skeletal muscle, we modified an ECM enrichment method from a previous study to optimize conditions for our samples and available equipment [37]. Skeletal muscle from N=6 sedentary, and N=5 exercise-trained male CD-1 mice was analyzed. Whole gastrocnemius muscle was pulverized in liquid nitrogen. Approximately 10 mg aliquots of pulverized muscle were homogenized (Tissuelyzer, Qiagen) in 30-fold volume per muscle weight (w/v; mg/μL) of a high salt buffer: 25 mM HEPES (pH 7.6), 300 mM NaCl, 0.2 % Rapigest (Waters Corporation) and 1X Halt™ Protease and Phosphatase Inhibitor Cocktail (Thermo Scientific). The homogenates were then

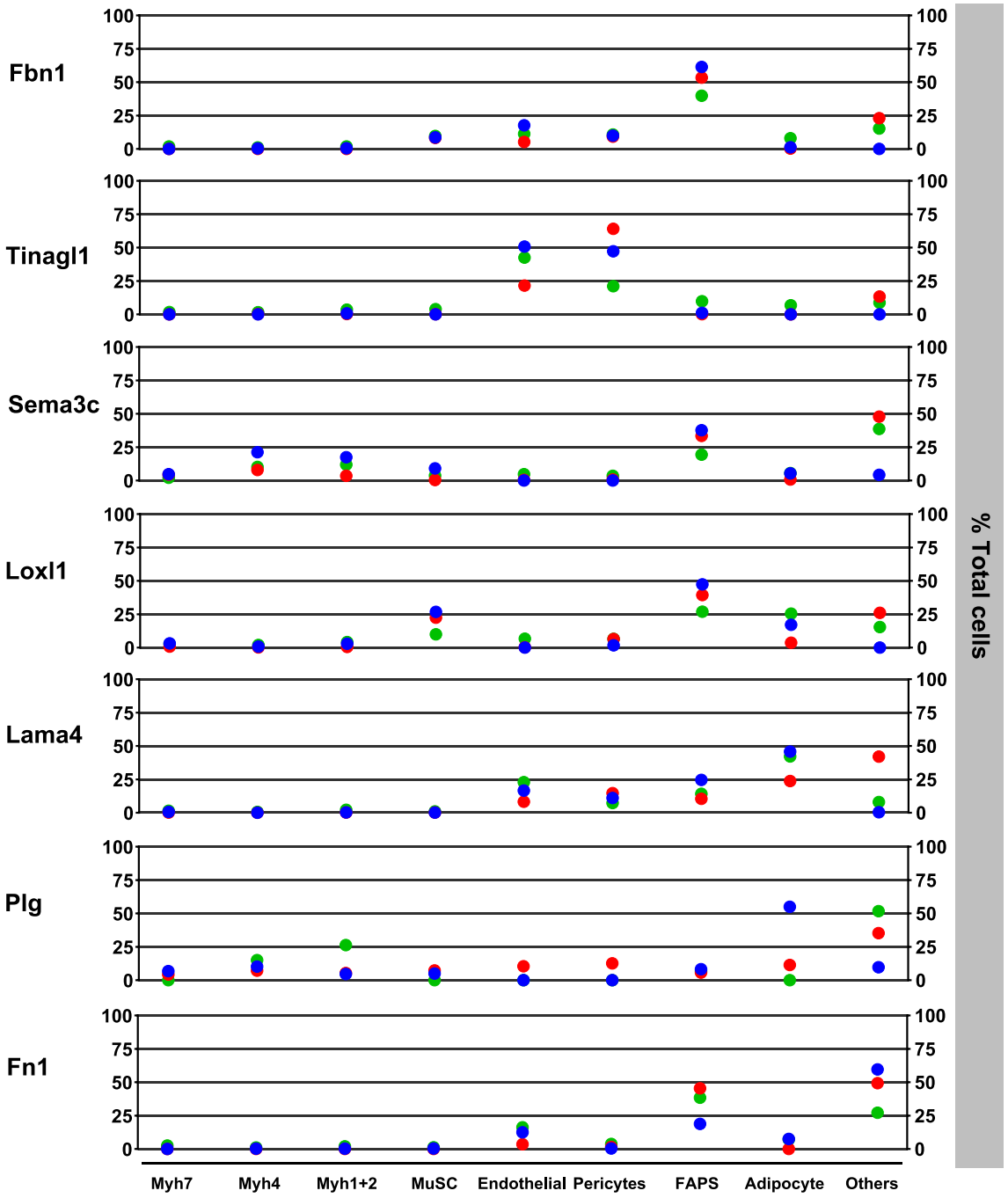

Fig. 7. ECM genes expressed in diverse cell types in skeletal muscle. ECM gene expression in each cell type was analyzed from 3 published single-nuclei RNA sequencing datasets. Each color represents percentage of gene expression in corresponding cell types from Dos et al. (blue), Wen et al. (red) and Petrany et al. (green). Myh7, Type 1 myofibers; Myh4, Type 2B myofibers; Myh1 + 2, Type 2A/X/D myofibers, FAPS, fibroadipogenic progenitor cells. (For interpretation of the references to color in this figure legend, the reader is referred to the web version of this article.)

centrifuged at 16,000 g for 30 min at 4°C to separate samples into soluble and insoluble fractions, which were derived from the supernatant and pellet, respectively.

For the insoluble fraction, the pellet was incubated in 30-fold volume (w/v; mg original muscle weight/μL) of pre-digestion enzyme: 1.35 mg/mL Liberase DH, 5 mM $CaCl_2$, 1 M TEAB. The pellets were incubated at 37 °C for 2 h under agitation, and were vortexed for 30 s every 30 min. The reaction was inactivated by adding EDTA to a final concentration of 20 mM. Protein concentrations were measured using a Pierce™ BCA Protein Assay Kit. 100 μg of insoluble protein from each sample was solubilized in 6 M urea in 100 mM TEAB by vortexing and 1-min sonication. Proteins were reduced in 5 mM DTT for 1 h at 37 °C, followed by alkylation in 25 mM chloroacetamide for 30 min at room temperature in dark. Proteins were then digested by 1 mg/mL Lys-C/trypsin (1:50) for 2 h at 37°C under agitation. Urea was reduced to a final concentration of 1 M by adding 100 mM TEAB. Proteins were further digested by 1 mg/mL Lys-C/trypsin (1:100) overnight at 37°C, under agitation. The reaction was inactivated by adding 50 % Trifluoroacetic acid (TFA) in water for a final pH≤2.

For the soluble fraction, Protein contents were measured by Pierce™ BCA Protein Assay Kit. 100 μg of proteins were reduced in 10 mM DTT for 30 min at 56°C, followed by alkylating in 60 mM chloroacetamide for

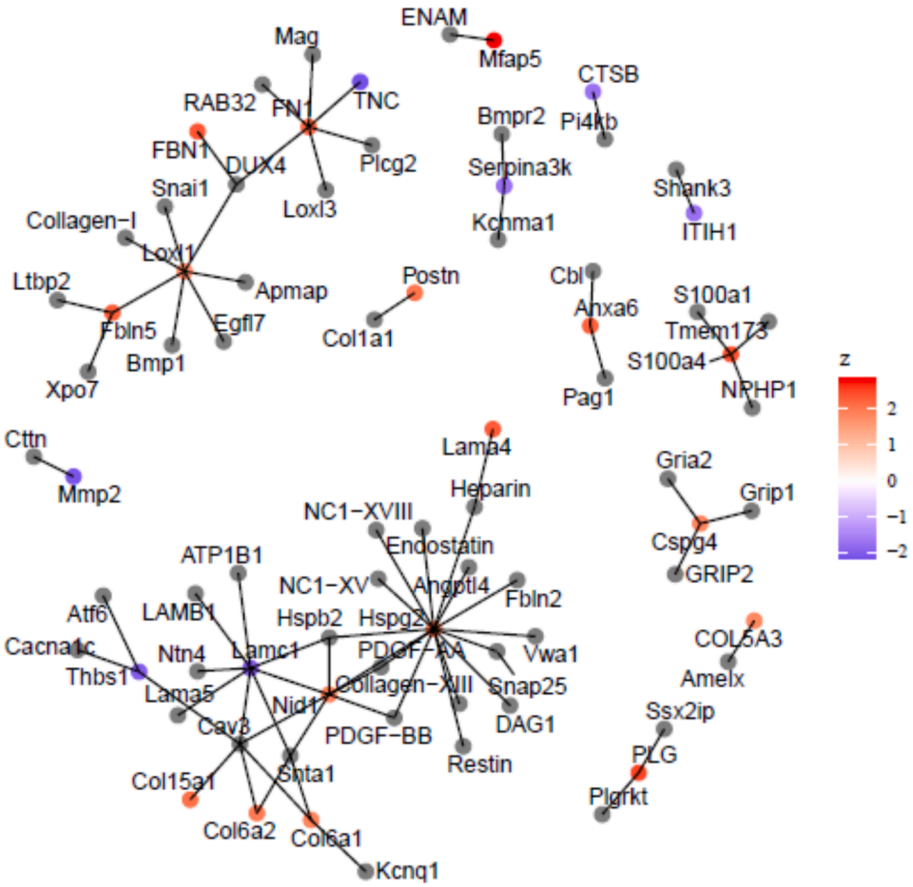

Fig. 8. Exercise regulation of ECM interaction networks. Interactome analysis demonstrates the complexity of ECM remodeling by exercise training. ECM proteins that were upregulated (red) or downregulated (blue) by exercise, may in-turn regulate large or small networks of both ECM and non-ECM proteins. Exercise-regulated proteins from our dataset are colored according to the z-score from exercise vs. control; others are colored gray. (For interpretation of the references to color in this figure legend, the reader is referred to the web version of this article.)

30 min at room temperature in the dark. To precipitate proteins, 9x volume of cold-ethanol was added and incubated overnight at 4°C, followed by centrifugation at 13,750g for 30 min at 4°C. Pellets were washed with 2 mL of ice-cold ethanol for 4 h at 4°C with constant rocking, followed by centrifugation at 13,750g for 30 min at 4°C. Pellets were then resuspended in 100 mM TEAB (pH 8) and digested by 1 mg/ml Lys-C/trypsin (1:25) overnight at 37°C, under agitation. The reaction was inactivated by adding 50% TFA in water for a final pH≤2.

Tandem mass tags for multiplexed proteomics

Peptides were processed for multiplexed proteomic analysis using a Tandem Mass Tag method [62].Digested peptides were desalted and quantified. Then, ~75 µg of peptides from each sample were labelled with Tandem Mass Tags (TMT). The ratio was verified by mixing ~ 5 µl of each TMT-labelled sample and analyzed by MS. After ratio verification, all TMT-labelled samples were combined, desalted and fractionated into 12 fractions by basic pH reversed-phase HPLC. All fractions were then analyzed by LC-MS3 [63]. The mouse Uniprot database was downloaded in May 2021. Peptide charge states used were 2–5. A flow chart summarizing our methodology is shown in Fig. 1.

Off-line basic pH reversed-phase (BPRP) fractionation. We fractionated the pooled, labeled peptide sample using BPRP HPLC [64] and an Agilent 1260 pump equipped with a degasser and a UV detector (set at 220 and 280 nm wavelength). Peptides were subjected to a 50-min linear gradient from 5% to 35% acetonitrile in 10 mM ammonium bicarbonate pH 8 at a flow rate of 0.6 mL/min over an Agilent 300Extend-C18 column (3.5 µm particles, 4.6 mm ID and 250 mm in length). The peptide mixture was fractionated into a total of 96 fractions, which were consolidated into 24 super-fractions [65], all of which were analyzed. Samples were subsequently acidified with 1% formic acid and vacuum centrifuged to near dryness. Each super-fraction was desalted via StageTip, dried again via vacuum centrifugation, and reconstituted in 5% acetonitrile, 5% formic acid for LC-MS/MS processing.

Liquid chromatography and tandem mass spectrometry. Mass spectrometric data were collected on Orbitrap Fusion Lumos instruments coupled to a Proxeon NanoLC-1200 UHPLC. The 100 µm capillary column was packed with 35 cm of Accucore 150 resin (2.6 µm, 150 Å; ThermoFisher Scientific) at a flow rate of ~ 400 nL/min. The scan sequence began with an MS1 spectrum (Orbitrap analysis, resolution 120,000, 400−1500 Th, automatic gain control (AGC) target 100%, maximum injection time "auto"). Data were acquired 180 min per fraction. MS2 analysis consisted of collision-induced dissociation (CID), quadrupole ion trap analysis, automatic gain control (AGC) $1x10^6$; NCE (normalized collision energy) 35, q-value 0.25, maximum injection time 35 ms), and isolation window at 0.7 Th. RTS was enabled and quantitative SPS-MS3 scans (resolution of 50,000; AGC target $2.5x10^5$; collision energy HCD at 50%, max injection time of 250 ms) were processed through Orbiter with a real-time false discovery rate filter implementing a modified linear discriminant analysis.

Data analysis. RAW files were searched using an in-house Comet-based platform. Searches were performed using a 50-ppm precursor ion tolerance for total protein level profiling. The product ion tolerance was set to 0.9 Da. Trypsin specificity was used. These wide mass tolerance

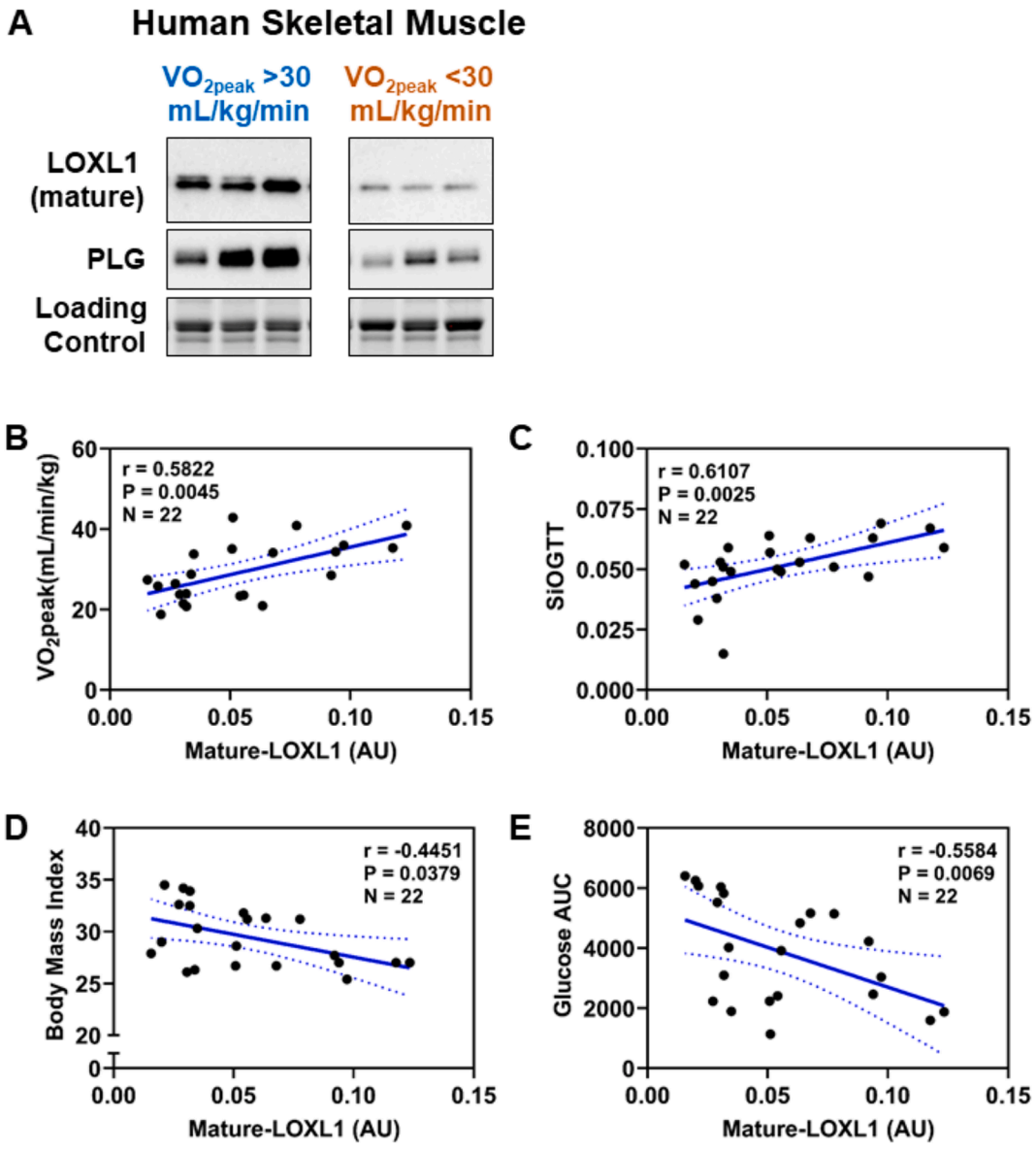

Fig. 9. Identification of LOXL1 in human skeletal muscle. (A) Muscle lysates from N=22 human participants were analyzed by Western blotting using antibodies against LOXL1 and plasminogen (PLG). Stain-free gel images (BioRad) are shown as a loading control. All samples were run and analyzed on the same gel/membrane. Mature LOXL1 protein was positively correlated with (B) aerobic exercise capacity (VO_2peak), and (C) insulin sensitivity determined during an oral glucose tolerance test (SiOGTT). Mature LOXL1 was negatively correlated with (D) body mass index, and (E) glucose area under the curve during an oral glucose tolerance test, with higher values indicating lower glucose tolerance. P-value <0.05 for Spearman correlation was considered statistically significant.

windows were chosen to maximize sensitivity in conjunction with Comet searches and linear discriminant analysis [66,67]. TMTpro labels on lysine residues and peptide N-termini + 304.207 Da), as well as carbamidomethylation of cysteine residues (+57.021 Da) were set as static modifications, while oxidation of methionine residues (+15.995 Da) was set as a variable modification. Peptide-spectrum matches (PSMs) were adjusted to a 1% false discovery rate (FDR) [68,69]. PSM filtering was performed using a linear discriminant analysis, as described previously [67] and then assembled further to a final protein-level FDR of 1% [69]. Proteins were quantified by summing reporter ion counts across all matching PSMs, also as described previously [70]. Reporter ion intensities were adjusted to correct for the isotopic impurities of the different TMTpro reagents according to manufacturer specifications. The signal-to-noise (S/N) measurements of peptides (extracted from the RAW file) assigned to each protein were summed and these values were normalized so that the sum of the signal for all proteins in each channel was equivalent to account for equal protein loading. Finally, each protein abundance measurement was scaled, such that the summed signal-to-noise for that protein across all channels equals 100, thereby generating a relative abundance (RA) measurement.

The mass spectrometry proteomics data have been deposited to the ProteomeXchange Consortium via the PRIDE [71] partner repository with the dataset identifier PXD053003.

Matrisome annotation and quantification

Only proteins with more than 50% non-missing values were kept. The remaining missing values were imputed using a random forest algorithm in the R package missForest [72]. The imputed values were normalized to have the same total intensity of all proteins and subsequently log2-transformed. Matrisome proteins were annotated by Matrisome annotator [16].

Proteins were tested for differential expression between exercise and control using moderated t-tests from the R package Limma [73]. Proteins with a p value <0.1 and fold change >1.2 were considered

differentially expressed. Due to the difficulty of cleaving ECM proteins, which have extensive post-translational modifications and cross-linking, we accepted targets with only 1 unique peptide detected. We tested association of protein abundance with exercise performance using Spearman rank correlation in R software.

Verification of exercise-induced muscle ECM remodeling protein targets

Western blotting

Using an independent cohort of N=12 sedentary and exercise-trained male mice, we sought to determine whether a subset of targets that were identified as differentially regulated by exercise using fractionation/MS could be detected and quantified using Western blotting methodology. Gastrocnemius muscle was pulverized in liquid nitrogen and homogenized in modified RIPA buffer (50 mM Tris-HCl (pH7.5), 10% (v/v) glycerol, 1% (v/v) Triton-X, 0.5% Sodium deoxycholate, 0.1% SDS, 1 mM EDTA, Halt™ Protease and Phosphatase Inhibitor Cocktail) by Tissuelyzer (Qiagen). Protein content was measured by Bradford assay (Bio-Rad). Equal concentrations of proteins from each sample were denatured in Laemmli buffer at 95 °C for 5 min and ~11.25 μg of protein was loaded into 4–20% Criterion™ TGX Stain-Free™ Protein Gel. Equal loading was verified by a stain-free image system (Bio-Rad). Proteins were transferred to nitrocellulose membrane by wet transfer with 10% methanol for FBN1 and LAMA4 and 20% methanol for other antibodies. Membranes were blocked for 1 h at room temperature with 3% BSA in TBST for FBN1 and LAMA4 and 5% non-fat dry milk in TBST for other antibodies. Membranes were then incubated in primary antibody against TINAGL1 (1:1000; 12077-1-AP, Proteintech), PLG (1:1000; ab154560, Abcam), LOXL1 (1:1000; PA5-87701, Invitrogen), SEMA3C (1:1000; PA5-90429, Invitrogen), FBN1 (1:1000; PA5-99225, Invitrogen) LAMA4 (1:1000; PA5-38938, Invitrogen) overnight at 4°C, followed by Anti-rabbit IgG (#7074, CST) secondary antibody incubation and visualization by chemiluminescence using a ChemiDoc Touch imaging system (Bio-rad). The band densities were quantified by Image Lab software (Bio-rad).

Muscle histology

Gastrocnemius muscle was dissected, immediately frozen in isopentane cooled by liquid nitrogen and stored at −80°C. Transverse sections of muscle were then cut at 7 μm thickness in a cryostat set at −20 °C. For fiber-typing, slides were incubated with primary antibodies against myosin heavy chain I (1:25; A4.840, DSHB) and myosin heavy chain IIa, (1:25; SC-71, DSHB) in TBS+1% BSA+1% NGS overnight at 4°C. After rinsing, mouse IgG1 fluorescent conjugate (A21124; red) and mouse IgM (A21042; green) secondary antibodies were added at 1:1000 in 1% BSA in TBS+1% NGS for 1 h. Wheat germ agglutinin (1:250; W6748, Invitrogen) was added with secondary antibodies for visualization of unstained fibers. For fibronectin, LAMA4, and griffonia lectin (capillary density), slides were fixed for 10 min with 10% Neutral Buffered Formalin (NBF) before staining. Antibodies against fibronectin (1:100; MA5-11981, Invitrogen) and LAMA4 (1:100; PA5-38938, Invitrogen) were applied overnight at 4 °C. Griffonia lectin (1:100; FL12015, Vectorlabs) was applied for 1 h at room temperature. Slides were imaged using EVOS M7000 imaging system and quantified using ImageJ/FIJI software.

Statistical analysis

All data presented as mean ± SD with individual values shown where appropriate. Mann-Whitney U Test was used to analyze differences between control (CON) and exercise training (ET) groups. Spearman's rank correlation coefficient was used to determine the relationship between ECM proteins and muscle remodeling phenotype.

ECM gene expression from single nucleus RNA-sequencing analysis

Single nucleus RNA-sequencing in mouse skeletal muscle from three datasets on NCBI GEO/SRA (GSE162307, GSE150065, GSE147127) were analyzed [32–34]. For all datasets, we downloaded the fastq files from SRA, generated gene UMI counts in droplets by aligning reads to the mouse genome (mm10) using the count function of 10x Genomics software Cell Ranger with the –include-introns option. Cell-containing droplets were distinguished using Monte Carlo simulations [74] and counts were normalized using SCTransform [75]. Cells were clustered using the Louvain algorithm, ambient RNA contamination was removed with DropletUtils [74], and doublets were removed with scDblFinder [76]. Samples were integrated with Seurat while keeping genes that are detected in at least 1 cell and cells where at least 1 gene is detected. We removed low quality cells that had too few UMI, too few features, or too high a percent of mitochondrial UMI (dying cells) from the integrated data. The integrated data were normalized with SCTransform [75] and clustered based on its 3000 most variable genes with the Louvain algorithm. To annotate cell types, we used SCSA [77] with the CellMarker reference database [78] or mouse muscle cell types as reported in Wen et al. 2021 [34] and Dos Santos et al. 2020 [32].

Matrisome interaction network analysis

The Extracellular Matrix Interaction Database (MatrixDB) [79] was searched for interactions involving the top ECM protein hits (those with $p < 0.1$) using their UniProt IDs. We removed self-loops and plotted the network using the R package ggraph which is based on the R package ggplot2.

Human participants

Characteristics of human participants were originally published in MacDonald et al., 2020 [51]. Additional analysis was performed using muscle lysates from these participants for Western blotting of ECM protein targets. Participants (11 male/13 female) were 24.5 ± 6.57 years old, did not have diagnosed metabolic disease (mean HbA1c 5.35 ±0.06 %), and had a body mass index of 29.55 ± 2.83 kg/m^2. Participants were considered sedentary and self-reported performing less than 150 min/week of moderate physical activity. Sufficient sample was available to perform ECM analysis on 22 of the 24 original study participants. Plasminogen and LOXL1 were quantified as described above for mouse Western blotting. Participants did not undergo an exercise training intervention prior to sample collection, and self-reported as performing less than 150 min per week of moderate to intense exercise. BMI, VO_2peak, glucose area under the curve (AUC), and the oral glucose tolerance test (OGTT)–derived insulin sensitivity (siOGTT) index were calculated as previously described and used for new correlation analysis with ECM markers in the present investigation. Written informed consent was obtained for all participants enrolled. The Joslin Diabetes Center Committee on Human Studies approved the study and its procedures.

CRediT authorship contribution statement

Pattarawan Pattamaprapanont: Writing – review & editing, Writing – original draft, Methodology, Investigation, Formal analysis, Data curation. **Eileen M. Cooney:** Writing – review & editing, Formal analysis, Data curation. **Tara L. MacDonald:** Writing – review & editing, Data curation. **Joao A. Paulo:** Writing – review & editing, Writing – original draft, Data curation. **Hui Pan:** Writing – review & editing, Formal analysis. **Jonathan M. Dreyfuss:** Writing – review & editing, Writing – original draft, Formal analysis. **Sarah J. Lessard:** Writing – review & editing, Writing – original draft, Supervision, Funding acquisition, Data curation, Conceptualization.

Declaration of competing interest

The authors declare that they have no known competing financial interests or personal relationships that could have appeared to influence the work reported in this paper.

Data availability

Data will be made available on request.

Acknowledgements

Tandem Mass Tags for Multiplexed Proteomics was performed by Thermo Fisher Scientific Center for Multiplexed Proteomics at Harvard Medical School. Research reported in this publication was supported by the National Institute of Diabetes and Digestive and Kidney Diseases grant R01 DK124258 (to SJL). Diabetes Research Center core facilities funded by National Institutes of Health, National Institute of Diabetes and Digestive and Kidney Diseases award number P30 DK036836. TLM was supported by a postdoctoral fellowship from the American Heart Association (19POST34381036). PP was supported by a Mary K. Iacocca Senior Visiting Fellowship.

Appendix A. Supplementary data

Supplementary data to this article can be found online at https://doi.org/10.1016/j.mbplus.2024.100159.

References

[1] B.K. Pedersen, M.A. Febbraio, Muscles, exercise and obesity: skeletal muscle as a secretory organ, Nat. Rev. Endocrinol. 8 (8) (2012) 457–465.
[2] F. Demontis, R. Piccirillo, A.L. Goldberg, N. Perrimon, The influence of skeletal muscle on systemic aging and lifespan, Aging Cell 12 (6) (2013) 943–949.
[3] B. Egan, J.R. Zierath, Exercise metabolism and the molecular regulation of skeletal muscle adaptation, Cell Metab. 17 (2) (2013) 162–184.
[4] D.L. Plotkin, M.D. Roberts, C.T. Haun, B.J. Schoenfeld, Muscle fiber type transitions with exercise training: shifting perspectives, Sports (basel) 9 (9) (2021).
[5] C.M. Bloor, Angiogenesis during exercise and training, Angiogenesis 8 (3) (2005) 263–271.
[6] B.K. Pedersen, B. Saltin, Exercise as medicine - evidence for prescribing exercise as therapy in 26 different chronic diseases, Scand. J. Med. Sci. Sports 25 (Suppl 3) (2015) 1–72.
[7] F. Draicchio, V. Behrends, N.A. Tillin, N.M. Hurren, L. Sylow, R. Mackenzie, Involvement of the extracellular matrix and integrin signalling proteins in skeletal muscle glucose uptake, J. Physiol. 600 (20) (2022) 4393–4408.
[8] H. Kim, M.C. Kim, H.H. Asada, Extracellular matrix remodelling induced by alternating electrical and mechanical stimulations increases the contraction of engineered skeletal muscle tissues, Sci. Rep. 9 (1) (2019) 2732.
[9] E. Kritikaki, R. Asterling, L. Ward, K. Padget, E. Barreiro, D.C.M. Simoes, Exercise training-induced extracellular matrix protein adaptation in locomotor muscles: a systematic review, Cells 10 (5) (2021).
[10] P. Pavan, E. Monti, M. Bondí, C. Fan, C. Stecco, M. Narici, et al., Alterations of extracellular matrix mechanical properties contribute to age-related functional impairment of human skeletal muscles, Int. J. Mol. Sci. 21 (11) (2020).
[11] R. Csapo, M. Gumpenberger, B. Wessner, Skeletal muscle extracellular matrix - what do we know about its composition, regulation, and physiological roles? A narrative review, Front. Physiol. 11 (2020) 253.
[12] T. Gustafsson, Vascular remodelling in human skeletal muscle, Biochem. Soc Trans. 39 (6) (2011) 1628–1632.
[13] L.R. Smith, E.R. Barton, Regulation of fibrosis in muscular dystrophy, Matrix Biol. 68–69 (2018) 602–615.
[14] A.S. Williams, L. Kang, D.H. Wasserman, The extracellular matrix and insulin resistance, Trends Endocrinol. Metab. 26 (7) (2015) 357–366.
[15] J.A. Timmons, E. Jansson, H. Fischer, T. Gustafsson, P.L. Greenhaff, J. Ridden, et al., Modulation of extracellular matrix genes reflects the magnitude of physiological adaptation to aerobic exercise training in humans, BMC Biol. 3 (2005) 19.
[16] A. Naba, K.R. Clauser, S. Hoersch, H. Liu, S.A. Carr, R.O. Hynes, The matrisome: in silico definition and in vivo characterization by proteomics of normal and tumor extracellular matrices, Mol Cell Proteom. 11 (4) (2012) M111.014647.
[17] P.A. Makhnovskii, V.G. Zgoda, R.O. Bokov, E.I. Shagimardanova, G.R. Gazizova, O. A. Gusev, et al., Regulation of proteins in human skeletal muscle: the role of transcription, Sci. Rep. 10 (1) (2020) 3514.
[18] H. Devos, J. Zoidakis, M.G. Roubelakis, A. Latosinska, A. Vlahou, Reviewing the regulators of COL1A1, Int. J. Mol. Sci. 24 (12) (2023).
[19] T.J. Mead, S. Bhutada, D.R. Martin, S.S. Apte, Proteolysis: a key post-translational modification regulating proteoglycans, Am. J. Physiol. Cell Physiol. 323 (3) (2022) C651–C655.
[20] S.D. Vallet, S. Ricard-Blum, Lysyl oxidases: from enzyme activity to extracellular matrix cross-links, Essays Biochem. 63 (3) (2019) 349–364.
[21] L.C. Olson, J.T. Redden, Z. Schwartz, D.J. Cohen, M.J. McClure, Advanced glycation end-products in skeletal muscle aging, Bioengineering (basel) 8 (11) (2021).
[22] M. Hostrup, A.K. Lemminger, B. Stocks, A. Gonzalez-Franquesa, J.K. Larsen, J. P. Quesada, et al., High-intensity interval training remodels the proteome and acetylome of human skeletal muscle, Elife (2022) 11.
[23] A. Byron, J.D. Humphries, M.J. Humphries, Defining the extracellular matrix using proteomics, Int. J. Exp. Pathol. 94 (2) (2013) 75–92.
[24] K.R. Jacobson, S. Lipp, A. Acuna, Y. Leng, Y. Bu, S. Calve, Comparative analysis of the extracellular matrix proteome across the myotendinous junction, J. Proteome Res. 19 (10) (2020) 3955–3967.
[25] A. Naba, K.R. Clauser, R.O. Hynes, Enrichment of extracellular matrix proteins from tissues and digestion into peptides for mass spectrometry analysis, J. vis. Exp. 101 (2015) e53057.
[26] D.R. Bassett Jr., E.T. Howley, Limiting factors for maximum oxygen uptake and determinants of endurance performance, Med. Sci. Sports Exerc. 32 (1) (2000) 70–84.
[27] S. van der Zwaard, F. Brocherie, R.T. Jaspers, Under the hood: skeletal muscle determinants of endurance performance, Front. Sports Act Living 3 (2021) 719434.
[28] Z.J. Wang, Q.W. Guan, H.H. Zhou, X.Y. Mao, F.H. Chen, Mechanistic insight into lysyl oxidase in vascular remodeling and angiogenesis, Genes Dis. 10 (3) (2023) 771–785.
[29] W. Zhang, Y. Liu, H. Zhang, Extracellular matrix: an important regulator of cell functions and skeletal muscle development, Cell Biosci. 11 (1) (2021) 65.
[30] A. Holland, S. Murphy, P. Dowling, K. Ohlendieck, Pathoproteomic profiling of the skeletal muscle matrisome in dystrophinopathy associated myofibrosis, Proteomics 16 (2) (2016) 345–366.
[31] N. Petajaniemi, M. Korhonen, J. Kortesmaa, K. Tryggvason, K. Sekiguchi, H. Fujiwara, et al., Localization of laminin alpha4-chain in developing and adult human tissues, J. Histochem. Cytochem. 50 (8) (2002) 1113–1130.
[32] M. Dos Santos, S. Backer, B. Saintpierre, B. Izac, M. Andrieu, F. Letourneur, et al., Single-nucleus RNA-seq and FISH identify coordinated transcriptional activity in mammalian myofibers, Nat. Commun. 11 (1) (2020) 5102.
[33] M.J. Petrany, C.O. Swoboda, C. Sun, K. Chetal, X. Chen, M.T. Weirauch, et al., Single-nucleus RNA-seq identifies transcriptional heterogeneity in multinucleated skeletal myofibers, Nat. Commun. 11 (1) (2020) 6374.
[34] Y. Wen, D.A. Englund, B.D. Peck, K.A. Murach, J.J. McCarthy, C.A. Peterson, Myonuclear transcriptional dynamics in response to exercise following satellite cell depletion, iScience 24 (8) (2021) 102838.
[35] J.W. Wragg, J.P. Finnity, J.A. Anderson, H.J. Ferguson, E. Porfiri, R.I. Bhatt, et al., MCAM and LAMA4 are highly enriched in tumor blood vessels of renal cell carcinoma and predict patient outcome, Cancer Res. 76 (8) (2016) 2314–2326.
[36] T.P. Solomon, S.K. Malin, K. Karstoft, S.H. Knudsen, J.M. Haus, M.J. Laye, et al., Association between cardiorespiratory fitness and the determinants of glycemic control across the entire glucose tolerance continuum, Diabetes Care 38 (5) (2015) 921–929.
[37] E. Ouni, S.P.D. Ruys, M.M. Dolmans, G. Herinckx, D. Vertommen, C.A. Amorim, Divide-and-Conquer Matrisome Protein (DC-MaP) Strategy: An MS-Friendly Approach to Proteomic Matrisome Characterization, Int J Mol Sci. 21 (23) (2020).
[38] A.S. Deshmukh, M. Murgia, N. Nagaraj, J.T. Treebak, J. Cox, M. Mann, Deep proteomics of mouse skeletal muscle enables quantitation of protein isoforms, metabolic pathways, and transcription factors, Mol Cell Proteomics. 14 (4) (2015) 841–853.
[39] A. Naba, K.R. Clauser, H. Ding, C.A. Whittaker, S.A. Carr, R.O. Hynes, The extracellular matrix: Tools and insights for the “omics” era, Matrix Biol. 49 (2016) 10–24.
[40] F.D. Lofaro, B. Cisterna, M.A. Lacavalla, F. Boschi, M. Malatesta, D. Quaglino, et al., Age-Related Changes in the Matrisome of the Mouse Skeletal Muscle, Int J Mol Sci. 22 (19) (2021).
[41] C.C. Yeung, A.T. Olesen, R. Wilson, S.R. Lamande, J.F. Bateman, R.B. Svensson, et al., Proteome profiles of intramuscular connective tissue: influence of aging and physical training, J. Appl. Physiol. (1985) 134 (5) (2023) 1278–1286.
[42] S.N. Blair, J.B. Kampert, H.W. Kohl 3rd, C.E. Barlow, C.A. Macera, R. S. Paffenbarger Jr, et al., Influences of cardiorespiratory fitness and other precursors on cardiovascular disease and all-cause mortality in men and women, J. Am. Med. Assoc. 276 (3) (1996) 205–210.
[43] S.N. Blair, H.W. Kohl 3rd, R.S. Paffenbarger Jr., D.G. Clark, K.H. Cooper, L. W. Gibbons, Physical fitness and all-cause mortality. A prospective study of healthy men and women, J. Am. Med. Assoc. 262 (17) (1989) 2395–2401.
[44] C. Bouchard, P. An, T. Rice, J.S. Skinner, J.H. Wilmore, J. Gagnon, et al., Familial aggregation of VO(2max) response to exercise training: results from the HERITAGE Family Study, J. Appl. Physiol. (1985) 87 (3) (1999) 1003–1008.
[45] C. Bouchard, T. Rankinen, Individual differences in response to regular physical activity, Med. Sci. Sports Exerc. 33 (6 Suppl) (2001) S446–S451, discussion S52–3.
[46] T.S. Church, M.J. LaMonte, C.E. Barlow, S.N. Blair, Cardiorespiratory fitness and body mass index as predictors of cardiovascular disease mortality among men with diabetes, Arch. Intern. Med. 165 (18) (2005) 2114–2120.
[47] K.J. Nadeau, J.G. Regensteiner, T.A. Bauer, M.S. Brown, J.L. Dorosz, A. Hull, et al., Insulin resistance in adolescents with type 1 diabetes and its relationship to cardiovascular function, J. Clin. Endocrinol. Metab. 95 (2) (2010) 513–521.

[48] K.J. Nadeau, P.S. Zeitler, T.A. Bauer, M.S. Brown, J.L. Dorosz, B. Draznin, et al., Insulin resistance in adolescents with type 2 diabetes is associated with impaired exercise capacity, J Clin Endocrinol Metab. 94 (10) (2009) 3687–3695.
[49] T.P. Solomon, S.K. Malin, K. Karstoft, J.M. Haus, J.P. Kirwan, The influence of hyperglycemia on the therapeutic effect of exercise on glycemic control in patients with type 2 diabetes mellitus, JAMA Intern. Med. 173 (19) (2013) 1834–1836.
[50] T.L. MacDonald, P. Pattamaprapanont, E.M. Cooney, R.C. Nava, J. Mitri, S. Hafida, et al., Canagliflozin Prevents Hyperglycemia-Associated Muscle Extracellular Matrix Accumulation and Improves the Adaptive Response to Aerobic Exercise, Diabetes 71 (5) (2022) 881–893.
[51] T.L. MacDonald, P. Pattamaprapanont, P. Pathak, N. Fernandez, E.C. Freitas, S. Hafida, et al., Hyperglycaemia is associated with impaired muscle signalling and aerobic adaptation to exercise, Nat Metab. 2 (9) (2020) 902–917.
[52] J.M. Robbins, B. Peterson, D. Schranner, U.A. Tahir, T. Rienmuller, S. Deng, et al., Human plasma proteomic profiles indicative of cardiorespiratory fitness, Nat Metab. 3 (6) (2021) 786–797.
[53] R. Yuan, Y. Li, B. Yang, Z. Jin, J. Xu, Z. Shao, et al., LOXL1 exerts oncogenesis and stimulates angiogenesis through the LOXL1-FBLN5/alphavbeta3 integrin/FAK-MAPK axis in ICC, Mol Ther Nucleic Acids. 23 (2021) 797–810.
[54] A.A. Ismail, B.T. Shaker, K. Bajou, The Plasminogen-Activator Plasmin System in Physiological and Pathophysiological Angiogenesis, Int J Mol Sci. 23 (1) (2021).
[55] F. Zhou, J. Sun, L. Ye, T. Jiang, W. Li, C. Su, et al., Fibronectin promotes tumor angiogenesis and progression of non-small-cell lung cancer by elevating WISP3 expression via FAK/MAPK/ HIF-1alpha axis and activating wnt signaling pathway, Exp Hematol Oncol. 12 (1) (2023) 61.
[56] F. Alonso, Y. Dong, L. Li, T. Jahjah, J.W. Dupuy, I. Fremaux, et al., Fibrillin-1 regulates endothelial sprouting during angiogenesis, Proc Natl Acad Sci U S a. 120 (23) (2023) e2221742120.
[57] Y. Sato, K. Kawashima, E. Fukui, H. Matsumoto, F. Yoshizawa, Y. Sato, Functional analysis reveals that Tinagl1 is required for normal muscle development in mice through the activation of ERK signaling, Biochim Biophys Acta Mol Cell Res. 1869 (9) (2022) 119294.
[58] G. Serini, L. Tamagnone, Bad vessels beware! Semaphorins will sort you out!, EMBO Mol Med. 7 (10) (2015) 1251–1253.
[59] H. Delavar, L. Nogueira, P.D. Wagner, M.C. Hogan, D. Metzger, E.C. Breen, Skeletal myofiber VEGF is essential for the exercise training response in adult mice, Am J Physiol Regul Integr Comp Physiol. 306 (8) (2014) R586–R595.
[60] M. Ross, C.K. Kargl, R. Ferguson, T.P. Gavin, Y. Hellsten, Exercise-induced skeletal muscle angiogenesis: impact of age, sex, angiocrines and cellular mediators, Eur J Appl Physiol. 123 (7) (2023) 1415–1432.
[61] J.M. Petrosino, V.J. Heiss, S.K. Maurya, A. Kalyanasundaram, M. Periasamy, R. A. LaFountain, et al., Graded Maximal Exercise Testing to Assess Mouse Cardio-Metabolic Phenotypes, PLoS One. 11 (2) (2016) e0148010.
[62] J. Navarrete-Perea, Q. Yu, S.P. Gygi, J.A. Paulo, Streamlined Tandem Mass Tag (SL-TMT) Protocol: An Efficient Strategy for Quantitative (Phospho)proteome Profiling Using Tandem Mass Tag-Synchronous Precursor Selection-MS3, J. Proteome Res. 17 (6) (2018) 2226–2236.
[63] L. Ting, R. Rad, S.P. Gygi, W. Haas, MS3 eliminates ratio distortion in isobaric multiplexed quantitative proteomics, Nat. Methods 8 (11) (2011) 937–940.
[64] Y. Wang, F. Yang, M.A. Gritsenko, Y. Wang, T. Clauss, T. Liu, et al., Reversed-phase chromatography with multiple fraction concatenation strategy for proteome profiling of human MCF10A cells, Proteomics 11 (10) (2011) 2019–2026.
[65] J.A. Paulo, J.D. O'Connell, R.A. Everley, J. O'Brien, M.A. Gygi, S.P. Gygi, Quantitative mass spectrometry-based multiplexing compares the abundance of 5000 S. cerevisiae proteins across 10 carbon sources, J. Proteomics 148 (2016) 85–93.
[66] S.A. Beausoleil, J. Villen, S.A. Gerber, J. Rush, S.P. Gygi, A probability-based approach for high-throughput protein phosphorylation analysis and site localization, Nat. Biotechnol. 24 (10) (2006) 1285–1292.
[67] E.L. Huttlin, M.P. Jedrychowski, J.E. Elias, T. Goswami, R. Rad, S.A. Beausoleil, et al., A tissue-specific atlas of mouse protein phosphorylation and expression, Cell 143 (7) (2010) 1174–1189.
[68] J.E. Elias, S.P. Gygi, Target-decoy search strategy for mass spectrometry-based proteomics, Methods Mol. Biol. 604 (2010) 55–71.
[69] J.E. Elias, S.P. Gygi, Target-decoy search strategy for increased confidence in large-scale protein identifications by mass spectrometry, Nat. Methods 4 (3) (2007) 207–214.
[70] G.C. McAlister, E.L. Huttlin, W. Haas, L. Ting, M.P. Jedrychowski, J.C. Rogers, et al., Increasing the Multiplexing Capacity of TMTs Using Reporter Ion Isotopologues with Isobaric Masses, Anal. Chem. 84 (17) (2012) 7469–7478.
[71] Y. Perez-Riverol, J. Bai, C. Bandla, D. García-Seisdedos, S. Hewapathirana, S. Kamatchinathan, et al., The PRIDE database resources in 2022: a hub for mass spectrometry-based proteomics evidences, Nucleic Acids Res. 50 (D1) (2021) D543–D552.
[72] D. Stekhoven, P. Bühlmann, MissForest–non-parametric missing value imputation for mixed-type data, Bioinformatics (Oxford, England). 28 (1) (2012) 112–118.
[73] M. Ritchie, B. Phipson, D. Wu, Y. Hu, C. Law, W. Shi, et al., limma powers differential expression analyses for RNA-sequencing and microarray studies, Nucleic Acids Res. 43 (7) (2015) gkv007-e47.
[74] A.T.L. Lun, S. Riesenfeld, T. Andrews, T.P. Dao, T. Gomes, J.C. Marioni, EmptyDrops: distinguishing cells from empty droplets in droplet-based single-cell RNA sequencing data, Genome Biol. 20 (1) (2019) 63.
[75] C. Hafemeister, R. Satija, Normalization and variance stabilization of single-cell RNA-seq data using regularized negative binomial regression, Genome Biol. 20 (1) (2019) 296.
[76] P.L. Germain, A. Lun, C. Garcia Meixide, W. Macnair, M.D. Robinson, Doublet identification in single-cell sequencing data using scDblFinder, F1000Res 10 (2021) 979.
[77] Y. Cao, X. Wang, G. Peng, SCSA: A Cell Type Annotation Tool for Single-Cell RNA-seq Data, Front. Genet. 11 (2020) 490.
[78] X. Zhang, Y. Lan, J. Xu, F. Quan, E. Zhao, C. Deng, et al., Cell Marker: a manually curated resource of cell markers in human and mouse, Nucleic Acids Res. 47 (D1) (2019) D721–D728.
[79] O. Clerc, M. Deniaud, S.D. Vallet, A. Naba, A. Rivet, S. Perez, et al., MatrixDB: integration of new data with a focus on glycosaminoglycan interactions, Nucleic Acids Res. 47 (D1) (2019) D376–D381.